The mechanism of the anti-inflammatory effect of Oldenlandia diffusa on arthritis model rats: a quantitative proteomic and network pharmacologic study

Hao Zhu[1]^, Xin-Gui Xiong[2,3]^, Ying Lu[4], Hui-Chun Wu[5], Zhi-Hui Zhang[1], Mei-Juan Sun[1]

[1]Department of Traditional Chinese Medicine, The First Affiliated Hospital of Soochow University, Soochow University, Suzhou, China; [2]Institute of Combined Traditional Chinese and Western Medicine, Xiangya Hospital, Central South University, Changsha, China; [3]National Clinical Research Center for Geriatric Disorders, Changsha, China; [4]Department of General Practice, Dushu Lake Hospital, Soochow University, Suzhou, China; [5]Department of Infectious Disease, The First Affiliated Hospital of Soochow University, Soochow University, Suzhou, China

Contributions: (I) Conception and design: XG Xiong, H Zhu; (II) Administrative support: None; (III) Provision of study materials or patients: XG Xiong, H Zhu; (IV) Collection and assembly of data: Y Lu, HC Wu; (V) Data analysis and interpretation: ZH Zhang, MJ Sun; (VI) Manuscript writing: All authors; (VII) Final approval of manuscript: All authors.

Correspondence to: Xin-Gui Xiong. Institute of Combined Traditional Chinese and Western Medicine, Xiangya Hospital, Central South University, Changsha, China. Email: xiongxg07@csu.edu.cn.

Background: In China, Oldenlandia diffusa (OD) has been prescribed as a therapeutic herb for rheumatoid arthritis (RA). We previously conducted a preliminary study of the anti-inflammatory effect of OD, and the purpose of this study is to further investigate its mechanism.

Methods: We performed a quantitative proteomic analysis of synovium, identified the differentially expressed proteins, and performed bioinformatics analyses. With the help of network pharmacology, we aimed to find the key synovial proteins which OD or its key compound might influence. To verify the result, liquid chromatography-mass spectrometry (LC-MS) was applied to quantify and qualify the absorbable potential compounds of OD. The anti-inflammatory effect was evaluated by morphological, histopathological, and cytokine analyses. Target proteins were observed by immunohistochemistry (IHC) and enzyme-linked immunosorbent assay (ELISA).

Results: MMP3 and CAV1 were identified as 2 of the differentially expressed proteins in RA synovium, and might be influenced by quercetin, the active compound of OD. MMP3 might be altered through atherosclerosis signaling, while CAV1 might be altered through caveolar-mediated endocytosis signaling. According to our verification, quercetin was identified as the absorbed and effective compound of OD, and it could exert an anti-inflammatory effect on the collagen-induced arthritis (CIA) model, including serum cytokine expression, synovial hyperplasia and lymphocyte infiltration, articular cartilage lesion. Quercetin could also down-regulate the synovial expression of MMP3 and CAV1, and could exert better effects at a high dose.

Conclusions: Quercetin was the main active compound of OD in the treatment of RA. OD might alleviate inflammatory responses in CIA rats by suppressing the expression of MMP3 and CAV1 through quercetin, and at a high dose, quercetin could exert a better anti-inflammatory effect.

Keywords: Isobaric tags for relative and absolute quantification (iTRAQ); network pharmacology; Oldenlandia diffusa (OD); rheumatoid arthritis

Submitted Jun 14, 2022. Accepted for publication Aug 30, 2022.
doi: 10.21037/atm-22-3678
View this article at: https://dx.doi.org/10.21037/atm-22-3678

^ ORCID: Hao Zhu, 0000-0003-4138-5624; Xin-Gui Xiong, 0000-0003-2566-4527.

Introduction

Rheumatoid arthritis (RA) is an inflammatory autoimmune disease which could exert adverse effects on the quality of life of patients. The clinical manifestations of RA include joint swelling, malfunction, and dysfunction (1). Among all pathological changes, synovitis and vasculitis play key roles (2) and can generate a series of inflammatory responses, involving a series of inflammatory pathways and cytokines (3). During the pathological process of RA, many proteins are differentially expressed. Some of them are vital and some are collateral. To determine the key proteins relevant to synovitis and vasculitis, here we employed collagen-induced arthritis (CIA) rats and applied isobaric tags for relative and absolute quantification (iTRAQ), a proteomics analysis method, to identify and evaluate the differentially expressed proteins (DEPs) and relevant information in the synovium of CIA rats.

The CIA model is a well-established model, with significant similarity to RA (4). Due to the elicitation of an artificial immune response and histopathological changes in the joints, especially the characterization of severe lymphocytes and pannus infiltration in synovial tissue and cartilage damage (4), the CIA model has been considered a suitable model for the study of RA and is extensively applied to study the pathogenesis of RA (5).

In recent years, quantitative proteomic techniques associated with iTRAQ have constantly been applied in biomedicine (6). To identify proteins in the procedure of iTRAQ analysis, proteins are tagged for the further labeling of most peptides. Meanwhile, with the help of iTRAQ, multiplexing is available in 4–8 different tags to compare proteins simultaneously in different groups (7). Ingenuity pathway analysis (IPA) is a powerful tool with multipurpose solutions for the interpretation, and the analysis of complicated experimental datasets (8). It has also been used by many scientific research institutions (9), including medical, pharmaceutical, and biotechnological institutions, among others. Based on this, iTRAQ quantitative proteomics associated with IPA analytical tool can offer a credible biological analysis of RA (10) by comparing different groups, especially could help us to reveal the key up-regulated or down-regulated DEPs.

In China, herbal medicines were widely prescribed as alternative medications to treat RA patients, and prescriptions consisting of multiple herbs usually exert a beneficial effect. However, the underlying mechanism of this effect still requires further research, and such knowledge is highly necessary as clinical therapeutic evidence. Considering that one herb contains multiple active compounds, and one prescription is usually formulated by multiple herbs, it is therefore complicated to focus on one complex prescription. Based on this, to elucidate the mechanisms and active compounds, our investigations start from one single herb. Oldenlandia diffusa (OD) plays a key role in the herbal prescriptions for RA, and it has been shown to have immunomodulatory activity (11). We previously showed that OD has an anti-inflammatory effect on CIA rats (12). Taken into consideration that OD contains multiple compounds (13), such as ferulic acid, p-coumaric, and quercetin, among others, it is unknown how these effective compounds play their roles, as well as which targets these compounds influence or which pathways they participate in. Therefore, by reflecting on our previous study, we have modified our approach to perform further investigations using network pharmacology.

With the rapid development of computer technology, the systematic pharmacological approach involving active compound screening, target prediction, and pathway analysis has been widely employed, especially in regards to natural herbs (14). Network pharmacology develops as an efficient tool which can systematically reveal the constitution and mechanism of complex biological progress (15), and has been commonly applied to traditional Chinese herbs to find potential targets and mechanisms (16,17). Through this method, regulating progress by small molecules can be clearly revealed (18). Therefore, we employed network pharmacology to study the relationship of herbal drug-targets in observing the key pathological changes of RA and aimed to find the therapeutic mechanism of OD.

In this study, we focused our attention on the key pathological changes in RA, synovitis and vasculitis, and narrowed our scope to one single effective herb, namely OD. We aimed to reveal the anti-inflammatory mechanism of OD in order to provide insights for further analyses on the treatment of RA by traditional Chinese medicine (TCM). We present the following article in accordance with the ARRIVE reporting checklist (available at https://atm.amegroups.com/article/view/10.21037/atm-22-3678/rc).

Methods

Ethical statement

Animal experiments were performed under a project license (No. SUDA20220613A01) granted by Ethics Committee of Soochow University, in compliance with the national guidelines for the care and use of animals.

iTRAQ analysis

To determine the DEPs in synovitis in the RA model, the iTRAQ technique was applied to analyze and compare synovium between CIA rats and control rats.

Animals

Healthy Sprague Dawley (SD) rats (n=80; 40 males, 40 females; 6–7 weeks old; 120±30 g; clean grade) Laboratory Animal Center of Soochow University. Five rats were housed per cage and all rats received food and water ad libitum under controlled environmental conditions (room temperature 20±3 ℃, room humidity 40–60%, background noise 40±10 dB, 12:12 h light-dark cycles) for 1 week to adapt to the environment. A protocol was prepared before the study without registration. A total of 80 rats were divided into the control group and the model group randomly (40 for the control group, 40 for the model group, with random and equal gender selection).

Induction and assessment of CIA

CIA model was established according to the guideline (Chondrex, Inc. 16928 Woodinville-Redmond Rd NE Suite B-101, Woodinville, WA 98072, USA). Bovine type II collagen (BIIC, 2 mg/mL, Chondrex, Inc. Immunization) was blended with Complete Freund's adjuvant (CFA, 10 mL, Sigma-Aldrich) or incomplete Freund's adjuvant (IFA, 10 mL, Sigma-Aldrich). On day 1, each rat was injected hypodermically on the base of the tail with 0.2 mL of the BIIC and CFA emulsion for the primary immunization. On day 7, each rat was given 0.1 mL of the BIIC and IFA emulsion for the booster immunization in the same way. On day 28, the posterior limbs of the rats were amputated, and synoviums from the knee joint were dissected and extracted for iTRAQ analysis.

DEP analysis

Trypsin digestion and iTRAQ labeling were carried according to the protocol from Applied Biosystems. In brief, 100 mg of protein was prepared in each pool, alkylated and digested overnight at 37 ℃. After checking the digestion by the Ultraflex TOF/TOF (Bruker, Germany), each sample from the control group and CIA group was labeled with iTRAQ reagents, mixed, and dried before further analyses. During labeling, the efficiency was calculated, which beyond 97%. After labeling, the peptides were fractionated through an SCX column (Luna SCX 100A, Phenomenex). Each sample labeled with iTRAQ was diluted with buffer A (25% acetone, pH 3.0, 10 mM KH_2PO_4). The fractionation was carried out by a linear binary gradient of 0–100% buffer B (25% acetone, 10 mM KH_2PO_4, 2 M KCl, pH 3.0) at a low rate, 1 mL/min, and analyzed on liquid chromatography column (Strata-X C18 column, 5 mm, 100 ×75 mm, 300 A, Phenomenex). Then, each sample was analyzed by high performance liquid chromatography (HPLC) with the gradient from 5% to 30% for 65 min at the rate of 400 mL/min, and further detected by Q Exactive LC-MS (Thermo Scientific). Subsequently, the result was identified for data acquisition and quantification. During this, Mascot software (version 2.3.0, Matrix Science, London, UK) and the Uniprot database (http://www.uniprot.org/) were applied to identify proteins. The protein quantitative ratio was compared and calculated, and was standardized in the average ratio of each label. The DEPs were presented with criteria: peptide matches ≥3, identified protein replication =3, ratio-fold change ≥1.3 or ≤–1.3, with P value <0.05.

Bioinformatics analysis of DEPs

We further analyzed the biological functions of DEPs, their pathways, and their associated networks. The data packet with ratio changes was uploaded into IPA, and identified in the Ingenuity Pathway Knowledge Base, and the involved pathways were also analyzed, with a criterion of P value <0.05.

Network construction and analysis

To find the potential molecular mechanism of OD, using the result from iTRAQ analysis we established the herb-compound-target network. First, we searched the active, absorbable components of OD through the Traditional Chinese Medicine Systems Pharmacology (TCMSP; https://old.tcmsp-e.com/tcmsp.php) database and analysis platform. With the default condition (OB >30%, DL >0.18), we searched for arthritis relevant information through literature and filtered the potential compounds to remove the irrelevant ones. We filtered for the active compounds which might have an anti-inflammatory effect on RA. We then recorded the corresponding targets and visualized the herb-compound-target network using Cytoscape 3.8.2 (http://www.cytoscape.org). Second, in order to find the targets relevant to the key pathological changes in RA, we searched and recorded the relevant targets through GeneCards (http://www.genecards.org/), OMIM (https://www.omim.org), and DisGeNet (https://www.disgenet.org) using the keywords "synovitis, vasculitis" and "rheumatoid

arthritis". Third, we intersected the results between the first part and the second part, then further intersected with DEPs, and drew the target and its relevant compound.

Analysis of absorbable compounds in OD

After the potential targets were revealed from network construction, we applied LC-MS to analyze whether the potential compounds from OD can be absorbed into plasma to prepare for further experiments.

Animals

SD rats (n=12, with random and equal gender selection; 6-7 weeks old; 120±30 g) were provided by the Laboratory Animal Center of Soochow University (animal housing condition was the same as iTRAQ analysis). A protocol was prepared before the study without registration. Rats were divided into 2 groups, namely the control group (n=6) and drug group (n=6).

Sample preparation

We prepared the OD decoction (30 g OD boiled in 500 mL water for 30 min) for subsequent experiments. Then, the OD daily dose was calculated and converted from human (0.43 g/kg, crude drug/weight, by assuming a regular weight of 70 kg) to rat (2.7 g/kg). Then, we fed the drug group with the OD decoction for 3 days according to the converted dose, while water was fed to the control group. On day 4, all rats were decapitated and their serum was extracted.

Qualitative determination of absorbable compounds in OD

The OD decoction and serum samples from the 2 groups were analyzed by LC-MS. We blended the sample (OD decoction, serum) with methyl alcohol, added 5 ml of 70% methanol solution, then shook and mixed the sample well. After being dissolved ultrasonically for 30 min, the samples were centrifuged then the upper liquid was extracted and put in a liquid phase vial to be tested. The LC-MS conditions were as follows: Agilent 1100; quadrupole-quadrapde-quadrupole-mass spectrometry API 4000, chromatographic column: Agilent Poroshell 120 ec-c18 2.7 μm (3×50 mm), mobile phase A: 0.5% formic acid water, mobile phase C: acetonitrile solution, flow rate: 0.6 mL/min, injection volume: 10 μL, column temperature: 35 ℃. For mass spectrometry detection, the multiple reaction monitoring (MRM) detection conditions were as follows: spray voltage 4.5–5.5 kV, desolvent temperature 500 ℃, desolvent gas (N2) 1,000 L/h. The mass spectrum scanning conditions were as follows: ESI+ (spray voltage 5.5 kV, desolvent temperature 500 ℃, desolvent gas (N2) 1,000 L/h, scanning range 100–1,000 m/z); ESI- (spray voltage 4.5 kV, desolvent temperature 500 ℃, desolvent gas (N2) 1,000 L/h, scanning range 100–1,000 m/z). Then, we acquired the total ion chromatogram (TIC) and extracted ion chromatogram (XIC), and according to the retention time and ion pair information, we could identify the absorbable compound in OD, plus its sub-ions.

Quantitative determination of absorbable compounds in OD

After we identified the compound, we dissolved the standard substance in methanol, in different concentrations of 0.625, 1.25, 2.5, 5 μg/mL, and analyzed them by LC-MS. According to the peak area of 2 different ions and their concentrations, we carried out the regression calculation via SPSS 26 and drew the regression curve using the equation Y=aX±b. Then, we calculated the concentration of the compound in the OD decoction and drug serum by the equation.

Observation of the effect of OD or its active compound on relevant targets

The potential absorbable compounds and their concentrations were revealed according to the result from LC-MS analysis. Then, we calculated the daily dose of the compounds for the rats. Meanwhile, based on the experiments in iTRAQ and network pharmacological analysis, the relevant targets could also be speculated. To verify whether the target protein can be altered by the active compound from OD, we administered the OD decoction or its compound to CIA rats and applied morphological analysis, histopathological analysis, and enzyme-linked immunosorbent assay (ELISA) to observe their anti-inflammatory effect, including the multiple dose effect of the compound. Lastly, we evaluated their effect on the relevant targets in synovium by immunohistochemistry (IHC) and ELISA.

Animals

SD rats (n=36; 18 males, 18 females; 6–7 weeks old; 120±30 g) were provided by the Laboratory Animal Center of Soochow University (animal housing condition was the same as iTRAQ analysis). A protocol was prepared before

the study without registration. Rats were divided into 3 groups, namely the intervention group (n=24), model group (n=6), and control group (n=6), with gender distributed randomly and equally. After primary (day 1) and booster (day 7) immunization (the procedure of CIA induction was the same as iTRAQ analysis), on day 14 the intervention group was divided into the active compound group (multiple dosages, n=18) and OD group (n=6) randomly, with gender distributed randomly and equally. The intervention group (subdivided into 3 different groups, 6 rats in each group, with gender distributed randomly and equally) received the active compound solution (3 different duplicated doses, each one for a single group) or OD decoction (at the regular dose) orally, while the same volume of purified water was administered to the control group and model group. On day 28, the posterior limbs of the rats were amputated, and serum and synovium from the knee joint were extracted.

Morphological analysis

On day 1, 14, 21, and 28, we observed the posterior limb of each rat, measured and record the arthritis index (AI). Joint morphological change was recorded in pictures, and AI was scored based on the degree of joint redness and swelling (19): 0= normal; 1= mild, but definite redness and swelling of the ankle, or apparent redness and swelling limited to individual digits, regardless of the number of affected digits; 2= moderate redness and swelling of the ankle; 3= severe redness and swelling of the entire paw including digits; and 4= maximally inflamed limb with involvement of multiple joints.

Histopathological analysis

On day 28, the rats were decapitated in batches, and their serum, synovium, and posterior limbs were extracted. According to the protocol, each sample was embedded in dehydrated paraffin, and sliced into 4 μm sections, then stained with hematoxylin-eosin (HE). Pathological changes from different groups were observed and compared under a microscope (magnified 10×, Leica DFC425C).

ELISA analysis

To observe the effect of OD or its active compound and the expression of relevant targets, we applied ELISA (Greenleaf, Co., Ltd. Suzhou, China) to analyze cytokines (TNF-α, IL-1β, IL-6) and the targets. Different samples were divided into groups (CIA group, compound group, OD group, and control group). Synovium was precooled and washed in PBS (0.02 mol/L, pH 7.0–7.2, 4 ℃), stored at –80 ℃, thawed at 4 ℃, and sufficiently homogenized. All samples were centrifuged at 1,000 r/min for 15 min in standby. The subsequent procedures were carried out according to the protocol from the kit's manual.

IHC analysis

After we amputated the posterior limbs of the rats, serial sections (4 mm) were sliced, rehydrated, and soaked in the solution of antigen retrieval (pH 6.0, 10 mmol/L sodium citrate buffer), and blocked endogenous peroxidase by 3% hydrogen peroxide in methanol for 20 min, and further blocked the nonspecific sites by 1% normal serum in phosphate for 20 min. Sections were incubated by anti-MMP3 (dilution 1:100) and anti-CAV1 (dilution 1:100), followed by avidin-biotin peroxidase complex. The tissue sections were incubated with 3,3-diaminobenzidine until a brown color developed, followed by counterstaining with hematoxylin. Immunostaining was evaluated by 2 blinded investigators.

Statistical analyses

We applied SPSS software (IBM, v26) to analyze the result from AI and ELISA. The results between groups were compared using two-way repeated measures analysis and the two-tailed independent *t*-test. Values of $P<0.05$ were considered significant.

Results

iTRAQ analysis

DEP analysis

After we compared the DEPs between the control group (40/40) and model group (40/40), 67 DEPs were identified above the ratio of 1.3 or below –1.3. Among these proteins, 40 were found to be up-regulated while 27 were down-regulated (*Table 1*) compared with the control group.

Bioinformatics of DEPs

A total of 154 DEPs were imported into IPA to determine the biological functions and canonical pathways. IPA included 3 primary categories: diseases and disorders, molecular and cellular functions, and physiological system development and functions. Among them, connective tissue disorders and inflammatory disease showed high significance (*Table 2*). This result confirmed that these DEPs

Table 1 Identification of differentially expressed proteins by iTRAQ-labeled quantitative proteomics

No.	Fold change	Symbol	Entrez gene name	Location	Type(s)
1	2.475	A1BG	Alpha-1-B glycoprotein	Extracellular space	Other
2	1.672	TNNC2	Troponin C type 2 (fast)	Cytoplasm	Other
3	1.608	PRELP	Proline/arginine-rich end leucine-rich repeat protein	Extracellular space	Other
4	1.602	COL5A2	Collagen, type V, alpha 2	Extracellular space	Other
5	1.586	Mug1/Mug2	Murinoglobulin 1	Extracellular space	Transporter
6	1.557	Ak1	Adenylate kinase 1	Cytoplasm	Kinase
7	1.507	MYH4	Myosin, heavy chain 4, skeletal muscle	Cytoplasm	Enzyme
8	1.496	S100A9	S100 calcium binding protein A9	Cytoplasm	Other
9	1.495	FTH1	Ferritin, heavy polypeptide 1	Cytoplasm	Enzyme
10	1.494	CA2	Carbonic anhydrase II	Cytoplasm	Enzyme
11	1.484	Mcpt1	Mast cell protease 1	Extracellular space	Peptidase
12	1.464	LIFR	Leukemia inhibitory factor receptor alpha	Plasma membrane	Transmembrane receptor
13	1.455	FN1	Fibronectin 1	Extracellular space	Enzyme
14	1.453	CA1	Carbonic anhydrase I	Cytoplasm	Enzyme
15	1.443	MYLPF	Myosin light chain, phosphorylatable, fast skeletal Muscle	Cytoplasm	Other
16	1.441	FNDC1	Fibronectin type III domain containing 1	Plasma membrane	Other
17	1.437	Kng1/Kng1l1	Kininogen 1	Extracellular space	Other
18	1.426	Pzp	Pregnancy zone protein	Extracellular space	Other
19	1.419	Lyz1/Lyz2	Lysozyme 2	Cytoplasm	Enzyme
20	1.402	Actn3	Actinin alpha 3	Plasma membrane	Other
21	1.4	MYL1	Myosin, light chain 1, alkali; skeletal, fast	Cytoplasm	Other
22	1.398	FTL	Ferritin, light polypeptide	Cytoplasm	Enzyme
23	1.394	ASPN	Asporin	Extracellular space	Other
24	1.388	Atp2a1	ATPase, Ca^{2+} transporting, cardiac muscle, fast twitch 1	Cytoplasm	Transporter
25	1.377	SERPINA6	Serpin peptidase inhibitor, clade A (alpha-1 antiproteinase, antitrypsin), member 6	Extracellular space	Other
26	1.373	LUM	Lumican	Extracellular space	Other
27	1.369	CA3	Carbonic anhydrase III, muscle specific	Cytoplasm	Enzyme
28	1.365	HBA1/HBA2	Hemoglobin, alpha 1	Cytoplasm	Transporter
29	1.351	APOE	Apolipoprotein E	Extracellular space	Transporter
30	1.348	HPX	Hemopexin	Extracellular space	Transporter
31	1.338	PRDX2	Peroxiredoxin 2	Cytoplasm	Enzyme
32	1.337	PLBD1	Phospholipase B domain containing 1	Extracellular space	Other
33	1.333	CMA1	Chymase 1, mast cell	Extracellular space	Peptidase
34	1.328	LIPA	Lipase A, lysosomal acid, cholesterol esterase	Cytoplasm	Enzyme

Table 1 (*continued*)

Table 1 (*continued*)

No.	Fold change	Symbol	Entrez gene name	Location	Type(s)
35	1.323	CD48	CD48 molecule	Plasma membrane	Other
36	1.321	CAV1	Caveolin 1, caveolae protein, 22 kDa	Plasma membrane	Transmembrane Receptor
37	1.316	PYGM	Phosphorylase, glycogen, muscle	Cytoplasm	Enzyme
38	1.307	MMP3	Matrix metallopeptidase 3 (stromelysin 1, progelatinase)	Extracellular space	Peptidase
39	1.303	ITIH4	Inter-alpha-trypsin inhibitor heavy chain family, member 4	Extracellular space	Other
40	1.303	S100A8	S100 calcium binding protein A8	Cytoplasm	Other
41	–1.3	RAB5A	RAB5A, member RAS oncogene family	Cytoplasm	Enzyme
42	–1.305	FKBP7	FK506 binding protein 7	Cytoplasm	Enzyme
43	–1.305	PPIC	Peptidylprolyl isomerase C (cyclophilin C)	Cytoplasm	Enzyme
44	–1.312	HEXB	Hexosaminidase B (beta polypeptide)	Cytoplasm	Enzyme
45	–1.332	IFIT1B	Interferon-induced protein with tetratricopeptide repeats 1B	Cytoplasm	Other
46	–1.337	RPS9	Ribosomal protein S9	Cytoplasm	Translation Regulator
47	–1.339	NARS	Asparaginyl-tRNA synthetase	Cytoplasm	Enzyme
48	–1.35	Sult1a1	Sulfotransferase family 1A, phenol-preferring, member 1	Cytoplasm	Enzyme
49	–1.35	TUBA1A	Tubulin, alpha 1a	Cytoplasm	Other
50	–1.351	STXBP1	Syntaxin binding protein 1	Cytoplasm	Transporter
51	–1.361	GSPT1	G1 to S phase transition 1	Cytoplasm	Translation regulator
52	–1.366	ENO2	Enolase 2 (gamma, neuronal)	Cytoplasm	Enzyme
53	–1.379	SPARC	Secreted protein, acidic, cysteine-rich (osteonectin)	Extracellular space	Other
54	–1.383	LGALS3BP	Lectin, galactoside-binding, soluble, 3 binding protein	Plasma membrane	Transmembrane receptor
55	–1.389	HIST1H1B	Histone cluster 1, H1b	Nucleus	Other
56	–1.439	HIBADH	3-hydroxyisobutyrate dehydrogenase	Cytoplasm	Enzyme
57	–1.441	C2	Complement component 2	Extracellular space	Peptidase
58	–1.445	BGN	Biglycan	Extracellular space	Other
59	–1.451	RPL18	Ribosomal protein L18	Cytoplasm	Other
60	–1.466	COL9A1	Collagen, type IX, alpha 1	Extracellular space	Other
61	–1.468	ACLY	ATP citrate lyase	Cytoplasm	Enzyme
62	–1.484	AP2S1	Adaptor-related protein complex 2, sigma 1 subunit	Cytoplasm	Transporter
63	–1.562	ACACA	Acetyl-CoA carboxylase alpha	Cytoplasm	Enzyme
64	–1.565	ATP1B1	ATPase, Na^+/K^+ transporting, beta 1 polypeptide	Plasma membrane	Transporter
65	–1.59	Fasn	Fatty acid synthase	Cytoplasm	Enzyme
66	–1.838	RETSAT	Retinol saturase (all-trans-retinol 13,14-reductase)	Cytoplasm	Enzyme
67	–1.98	KRT8	Keratin 8	Cytoplasm	Other

iTRAQ, isobaric tags for relative and absolute quantification.

Table 2 Top proteomic bio-functions of synovium analyzed by IPA along with the associated numbers of molecules and –log(P value)

Top bio functions	–log(P value)	Molecules
Diseases and disorders		
Cancer	2.11–9.91	33
Connective tissue disorders	2.02–5.97	11
Inflammatory disease	2.05–5.97	21
Skeletal and muscular disorders	2.02–5.97	25
Dermatological diseases and conditions	2.02–5.65	10
Molecular and cellular functions		
Cell morphology	2.02–8.27	48
Cellular assembly and organization	2.02–8.27	40
Cellular function and maintenance	2.02–7.32	44
Molecular transport	2.02–6.55	48
Carbohydrate metabolism	2.02–6.44	27
Physiological system development and function		
Hair and skin development and function	2.02–6.22	7
Tissue morphology	2.02–5.79	54
Embryonic development	2.02–5.67	30
Organ development	2.02–5.67	36
Organ morphology	2.02–5.67	50

IPA, ingenuity pathway analysis.

were specially related to the key pathological change in synovial tissue from CIA rats. Among the related molecular and cellular functions, plus with related tissue morphology from physiological system development and function, these characteristics indicated the key targets might pathologically change or exert their effects through these functions. Meanwhile, among all the canonical pathways identified by IPA (*Table 3*), 34 of them were significant (P value <0.05), with each one of them involving a series of DEPs. Based on these pathways, along with other conditions, we could speculate which one of these DEPs might be modulated by OD or its compounds, as well as the relevant pathways.

OD network construction and further analysis

After we recorded the relevant targets of 8 compounds from OD (p-MCA, deacetyl asperuloside acid, geniposidic acid, stigmasterol, beta-sitosterol, FER, p-coumaric acid, and quercetin, we uploaded the data into Cytoscape 3.8.2 to construct the herb-compound-target network. According to the result, we found that quercetin showed the widest relationship (*Figure 1*). Based on the search results through GeneCards, OMIM, and DisGeNet, we intersected the targets between "synovitis, vasculitis" and "RA" then further intersected them with the target of OD and DEPs, and found 2 potential targets (*Figure 2*), namely MMP3 and CAV1. The 2 proteins were relevant to the key pathological change of RA, and may also be affected by quercetin, the compound of OD. According to the results, we looked back at the expression of these 2 DEPs and found that they were up-regulated in CIA rats compared to control rats. MMP3 had a fold change of 1.307, while CAV1 had a fold change of 1.321. They may both be regulated by quercetin, which is an active compound of OD. We then looked up the pathway results determined by IPA and found 2 related significant pathways that might be involved (*Figure 3*): atherosclerosis signaling for MMP3 and caveolar-mediated endocytosis signaling for CAV1. These results showed that MMP3 and CAV1 might be the target proteins of quercetin, the compound of OD. We verified this result in the subsequent experiments.

Analytical performance of the absorbable compound in OD

Qualitative determination of the absorbable compound of OD

After we extracted the serum (6/6 for the control group, 6/6 for the drug group), the data comparison was carried by EasyTest Techology (ET-Tec. Ltd, Guangzhou, China), which was founded by the retention time and ion pair information from mixed samples. We input the information and retention time into the methodology file and determined the mass spectrometry performance of Que. Then, we applied MRM (negative ion mode) by triple quadrupole mass spectrometry. Representative chromatograms of quercetin and beta-sitosterol were shown for the mixed standard substance (*Figure 4*), OD decoction (*Figure 5*), and drug serum (*Figure 6*). The retention time of quercetin's ion pair (301.000/150.900 Da) emerged at the time of 9.95 min in XIC and TIC; meanwhile, beta-sitosterol's ion pair (415.000/73.000 Da) emerged at the time of 14.6 min. According to this, we confirmed that both quercetin and beta-sitosterol, the active compounds of OD, could be absorbed into blood after OD being taken orally.

Table 3 Relevant canonical pathways identified by IPA, in which those with –log(P value) >1.3 were selected, corresponding to P value <0.05

No.	Ingenuity canonical pathways	–log(P value)	Ratio	Molecules
1	LXR/RXR activation	4.89	0.07	APOE, PON1, HPX, ITIH4, ACACA, S100A8, A1BG, RBP4
2	Acute phase response signaling	4.54	0.05	PLG, HPX, FTL, HP, FN1, ITIH4, CP, C2, RBP4
3	Atherosclerosis signaling	4.00	0.06	APOE, PON1, MMP3, CMA1, COL2A1, S100A8, RBP4
4	Granzyme A signaling	3.12	0.16	Hist1h1d, APEX1, HIST1H1B
5	TR/RXR activation	2.93	0.06	HP, COL6A3, ACACA, G6PC, ME1
6	Clathrin-mediated endocytosis signaling	2.79	0.04	APOE, PON1, RAB5A, CLTA, S100A8, AP2S1, RBP4
7	Role of IL-17A in psoriasis	2.50	0.22	S100A9, S100A8
8	Remodeling of epithelial adherens junctions	2.45	0.06	TUBA1A, RAB5A, TUBA4A, Actn3
9	Actin cytoskeleton signaling	2.37	0.03	MYH4, TLN2, FN1, MYLPF, Actn3, GSN, MYL1
10	Calcium signaling	2.21	0.03	MYH4, TNNC2, TNNT3, Tpm1, MYL1, PRKAR1A
11	EIF2 signaling	2.08	0.03	RPL6, RPL4, RPL5, RPS9, Eif4a3, RPL18
12	Acetyl-CoA biosynthesis III (from Citrate)	2.02	1.00	ACLY
13	Asparagine biosynthesis I	2.02	1.00	ASNS
14	Glutathione redox reactions I	1.94	0.12	GPX3, GPX1
15	Epithelial adherens junction signaling	1.91	0.04	MYH4, TUBA1A, TUBA4A, Actn3, MYL1
16	Germ cell-sertoli cell junction signaling	1.80	0.03	TUBA1A, PPAP2B, TUBA4A, Actn3, GSN
17	Dopamine degradation	1.76	0.10	ALDH2, Sult1a1
18	Glycolysis I	1.65	0.08	PKM, ENO2
19	Gluconeogenesis I	1.65	0.08	ENO2, ME1
20	Sertoli cell-sertoli cell junction signaling	1.59	0.03	TUBA1A, PPAP2B, TUBA4A, Actn3, PRKAR1A
21	IL-12 signaling and production in macrophages	1.56	0.03	APOE, PON1, S100A8, RBP4
22	Protein kinase A signaling	1.56	0.02	MYH4, PYGM, MYLPF, Hist1h1d, APEX1, HIST1H1B MYL1, PRKAR1A
23	ILK signaling	1.52	0.03	MYH4, FN1, PPAP2B, Actn3, MYL1
24	Caveolar-mediated endocytosis signaling	1.49	0.04	RAB5A, CAV1, CD48
25	Cellular effects of sildenafil (viagra)	1.48	0.03	MYH4, MYLPF, MYL1, PRKAR1A
26	Complement system	1.45	0.06	CFD, C2
27	AMPK signaling	1.43	0.03	Ak1, CKM, ACACA, PRKAR1A
28	Creatine-phosphate biosynthesis	1.42	0.25	CKM
29	Phenylethylamine degradation I	1.42	0.25	ALDH2
30	Biotin-carboxyl carrier protein assembly	1.42	0.25	ACACA
31	Regulation of actin-based motility by Rho	1.39	0.04	MYLPF, GSN, MYL1
32	Neuroprotective role of THOP1 in Alzheimer's disease	1.33	0.05	PLG, PRKAR1A
33	FXR/RXR activation	1.32	0.04	APOE, PON1, G6PC
34	CTLA4 signaling in cytotoxic T lymphocytes	1.30	0.03	CLTA, HLA-DRA, AP2S1

IPA, ingenuity pathway analysis.

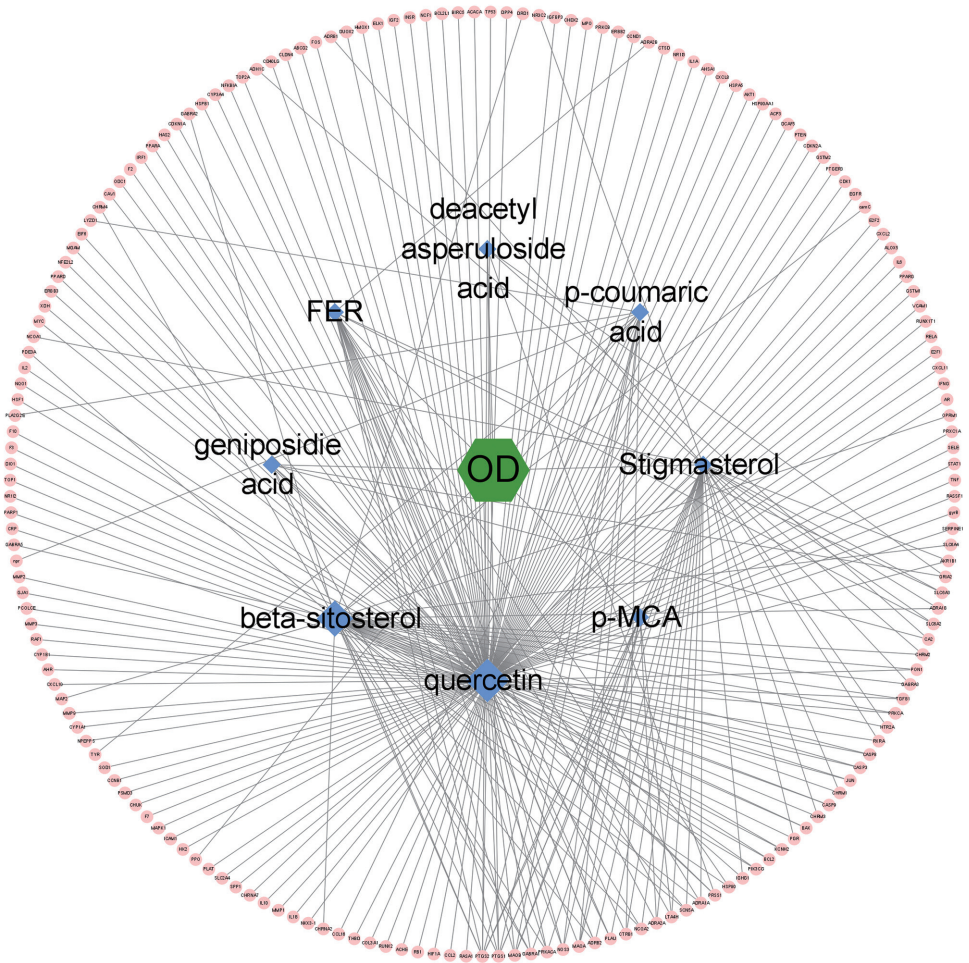

Figure 1 Herb-compound-target network. Green: OD; Blue: active compounds of OD; Pink: target proteins which were relevant to the active compounds. OD, Oldenlandia diffusa; FER, ferulic acid; p-MCA, 4-methoxycinnamic acid.

Quantitative determination of the absorbable compounds in OD

We confirmed that 2 of the potential compounds from OD, quercetin and beta-sitosterol, were absorbable. However, according to the iTRAQ and network pharmacologic studies, we found that only quercetin might regulate MMP3 and CAV1, which are strongly connected to inflammatory responses in the synovium. Based on this, we performed further experiments on quercetin and quantified its concentrations by MRM–. We analyzed another ion pair (301.000/178.900 Da) of quercetin, recorded the peak areas of the standards in 4 incremental concentrations, and drew the standard curve (*Figure 7*): Y=152083X+37304, with the coefficient of determination (R^2) at 0.9981. Then, we analyzed it by using a $1/X^2$ weighted linear regression and amended the curve to Y=160295.65X +22539, R^2=0.9985. The lower limit of quantitation (LLOQ), the low quantitation (LQ), the middle quantitation (MQ), and the high quantitation (HQ) of quercetin's standards were 0.625, 1.25, 2.5, and 5 μg/mL, respectively. Results showed that the intra- and inter-day precision and accuracy of standards of different concentrations were all reliable (*Table 4*). The intra- and inter-accuracy of the OD decoction and drug serum were also tested and found to be reliable (*Table 4*). Meanwhile, we assayed the stability of the OD decoction and drug serum (*Table 5*), and results showed that quercetin was stable in both samples after being stored at 4 ℃ for 0, 6, 12, and 24 h. The recovery rate of quercetin was also analyzed (*Table 5*). We added 80%, 100%, and 120% standard solutions to the OD decoction and drug serum, and results showed that the average recovery stay was between 2.7% to 7.38% (*Table 5*). According to the

results, we calculated that the concentration of quercetin in OD was 52.5 μg/g (compound/crude drug).

The effect of the OD decoction and its active compound quercetin on CIA rats

After we confirmed that quercetin, the potential compound of OD, could be absorbed into blood after being orally taken, we investigated if it might also play a key role in the anti-inflammatory effect in the synovium of CIA rats. Considering that some of the previous steps were based on speculation by network pharmacology, we verified the effect of quercetin on CIA rats. First, based on the regular dose of OD for humans (30 g/d, by assuming a regular weight of 70 kg), we calculated that the regular dose of OD for rats was 2.7 g/kg. According to the result from quantitative determination, we calculated that the daily dose of quercetin for rats was 0.28 mg/kg, but after we searched the detection of quercetin's concentration from other scholars' reference, we found our intervening dose of quercetin in OD stayed in a low level, plus this dose was regular, we used to prescribe OD for the patients in such dose. Because of this, to better observe its influence, we added the decuple and centuple concentrations of quercetin for intervention, which were 2.8 mg/kg (medium dose, MD) and 28 mg/kg (high dose, HD), respectively, plus with the detected regular dose, 0.28 mg/kg (low dose, LD), and OD decoction, respectively. On day 28, we extracted the serum, posterior limbs, and synovium from the control group (12/12), model group (12/12), OD group (12/12), Que-LD (quercetin in low dose) group (12/12), Que-MD (quercetin in medium dose) group (12/12), and Que-HD (quercetin in high dose) group (12/12).

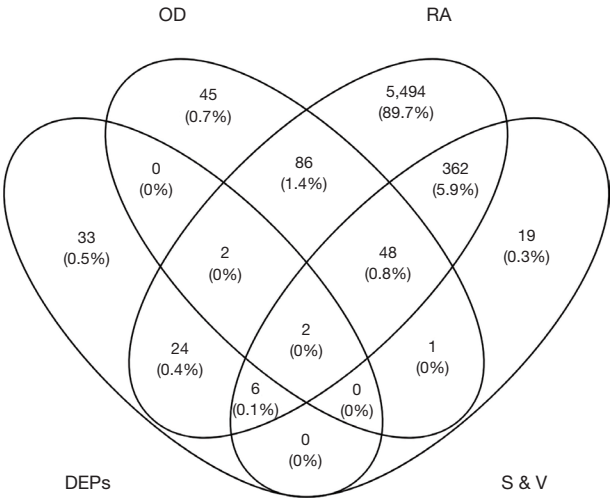

Figure 2 Intersected targets among the targets of DEPs, OD, RA, and S&V. Two were found to be related, namely MMP3 and CAV1. DEPs, differentially expressed proteins; OD, Oldenlandia diffusa; RA, rheumatoid arthritis; S&V, synovitis & vasculitis.

Morphological analysis

As shown in *Figure 8*, in the control group (*Figure 8A*), the

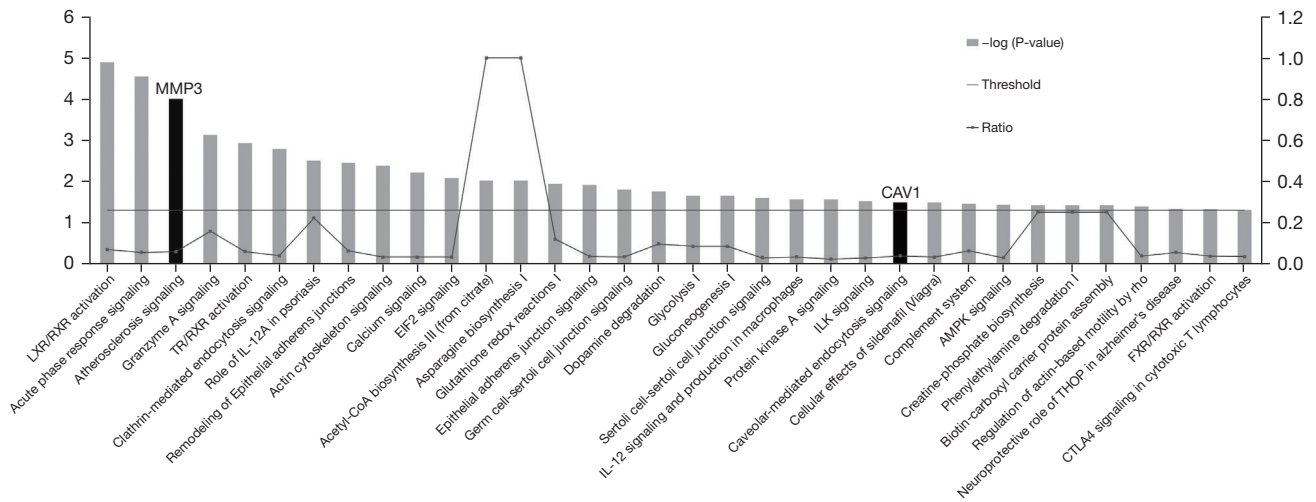

Figure 3 Canonical pathways associated with the 67 DEPs. Their expression was significant (threshold of 1.3 corresponds to P value of 0.05) as identified by IPA. Among them, 2 significant pathways were identified (black columns), namely atherosclerosis signaling for MMP3 and caveolar-mediated endocytosis signaling for CAV1. DEPs, differentially expressed proteins; IPA, ingenuity pathway analysis.

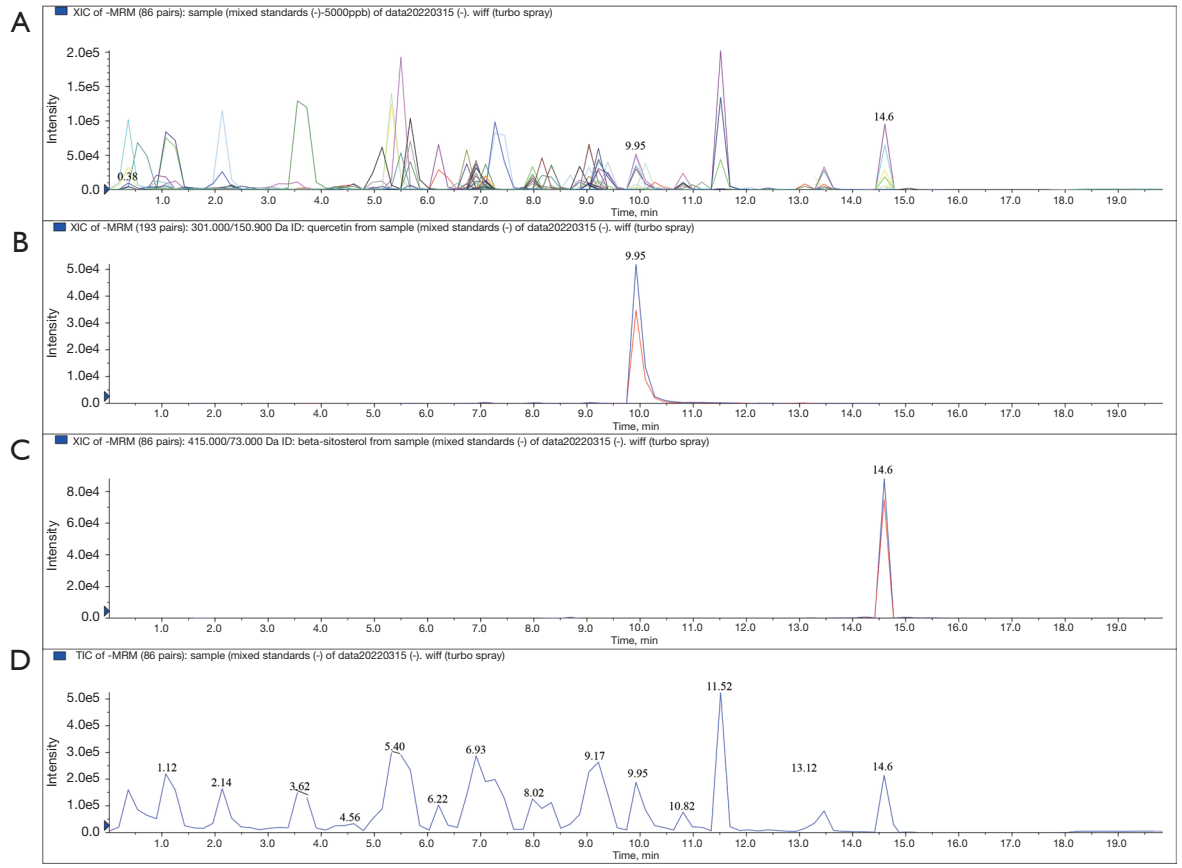

Figure 4 Ion chromatograms of the mixed standard substance by MRM in negative mode. (A) XIC of the mixed standard substance; (B) XIC of quercetin; (C) XIC of beta-sitosterol; (D) TIC of the mixed standard substance. MRM, multiple reaction monitoring; XIC, extracted ion chromatogram; TIC, total ion chromatogram.

posterior limb was slim and, and the skin color was pink. After the second immunization, swelling, redness, ankylosis, and hyperemia appeared on day 14 (*Figure 8B*). These morbidities deteriorated from day 21 (*Figure 8C*) to 28 (*Figure 8D*). After we intervened with OD decoction on day 15, minor alleviation were observed in terms of skin redness and ankle swelling on day 21 (*Figure 8E*), in comparison with the model group (*Figure 8C*). By day 28 (*Figure 8F*), ankle swelling and skin redness were alleviated compared to the model group (*Figure 8D*). After we intervened with Que-LD on day 14, minor alleviation were observed in terms of skin redness and ankle swelling on day 21 (*Figure 8G*) compared to the model group (*Figure 8C*). By day 28 (*Figure 8H*), although ankle swelling and skin redness was not as severe as in the model group (*Figure 8D*), but showed no significant alleviation compared to its prior appearance. After we intervened with Que-MD on day 14, minor alleviation were observed in terms of skin redness and ankle swelling on day 21 (*Figure 8I*) compared to the model group (*Figure 8C*). By day 28 (*Figure 8J*), alleviation of ankle swelling and skin redness were observed, compared to both the model group (*Figure 8D*) and its prior appearance. After we intervened with Que-HD on day 14, obvious alleviation in terms of skin redness and ankle swelling were observed on day 21 (*Figure 8K*), compared to the model group (*Figure 8C*). By day 28 (*Figure 8L*), notable alleviation in terms of ankle swelling and skin redness were observed, compared to the model group (*Figure 8D*), other quercetin groups (*Figure 8H,8J*), and its prior appearance.

As shown in *Figure 9*, after immunizations, the AI deteriorated from day 1 to 14 in each group. After interventions, from day 14–21, the rise in AI in the OD, Que-HD, and Que-MD groups were restrained compared with day 1–14, while it still showed a strong upward trend in the model and Que-LD groups. From day 21–28, AI decreased in the OD, Que-HD, and Que-MD groups

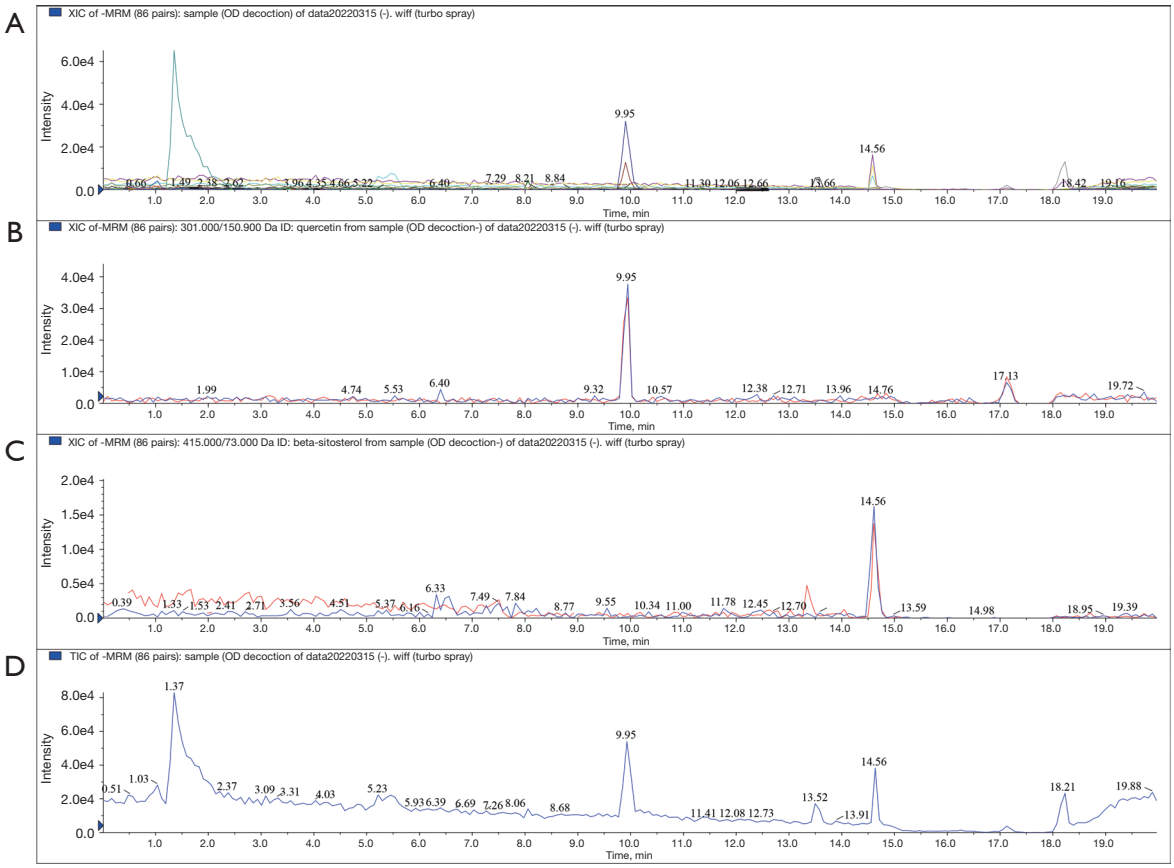

Figure 5 Ion chromatograms of the OD decoction by MRM in negative mode. (A) XIC of the OD decoction; (B) XIC of quercetin; (C) XIC of beta-sitosterol; (D) TIC of the OD decoction. OD, Oldenlandia diffusa; MRM, multiple reaction monitoring; XIC, extracted ion chromatogram; TIC, total ion chromatogram.

compared to their previous results, with a significant difference compared to the model group (P<0.05) on day 28, while Que-LD showed no difference. Among them, only the Que-HD group showed a significant difference compared with the OD group (P<0.05).

Histopathological analysis

As shown in *Figure 10*, in the control group (*Figure 10A*), regular scope (×40) showed articular cartilage was intact, the synovium was regular, with no hyperplasia or invasion, and there was a clear space between the joint. Meanwhile, magnified scope (×200) showed minor inflammatory cell and pannus infiltration in the synovium. Compared to the control group, in the model group (*Figure 10B*), regular scope (×40) showed articular cartilage was defective, the synovium displayed over-hyperplasia and infiltrated into cartilage, even merging with it, and no joint space was observed. Meanwhile, magnified scope (×200) showed significant lymphocyte and pannus infiltration in the synovium. In the OD group (*Figure 10C*), regular scope (×40) showed that a large part of the articular cartilage was intact, only small part of it was mildly impaired, with lymphocyte infiltration. Compared with the model group, a clear joint space was observed, and lymphocyte infiltration was alleviated. In the Que-LD group (*Figure 10D*), regular scope (×40) showed that a large part of the articular cartilage was impaired, the synovium displayed over-hyperplasia and infiltrated into cartilage, and compared with the model group, a narrow joint space was observed. Meanwhile, magnified scope (×200) showed that a large amount of lymphocytes infiltrated the synovium, with no obvious alleviation compared with the model group. In the Que-MD group (*Figure 10E*), regular scope (×40) showed that a large part of the articular cartilage was intact, and a small part of it was mildly invaded by synovium, with mild synovial hyperplasia. Compared with the model group, a

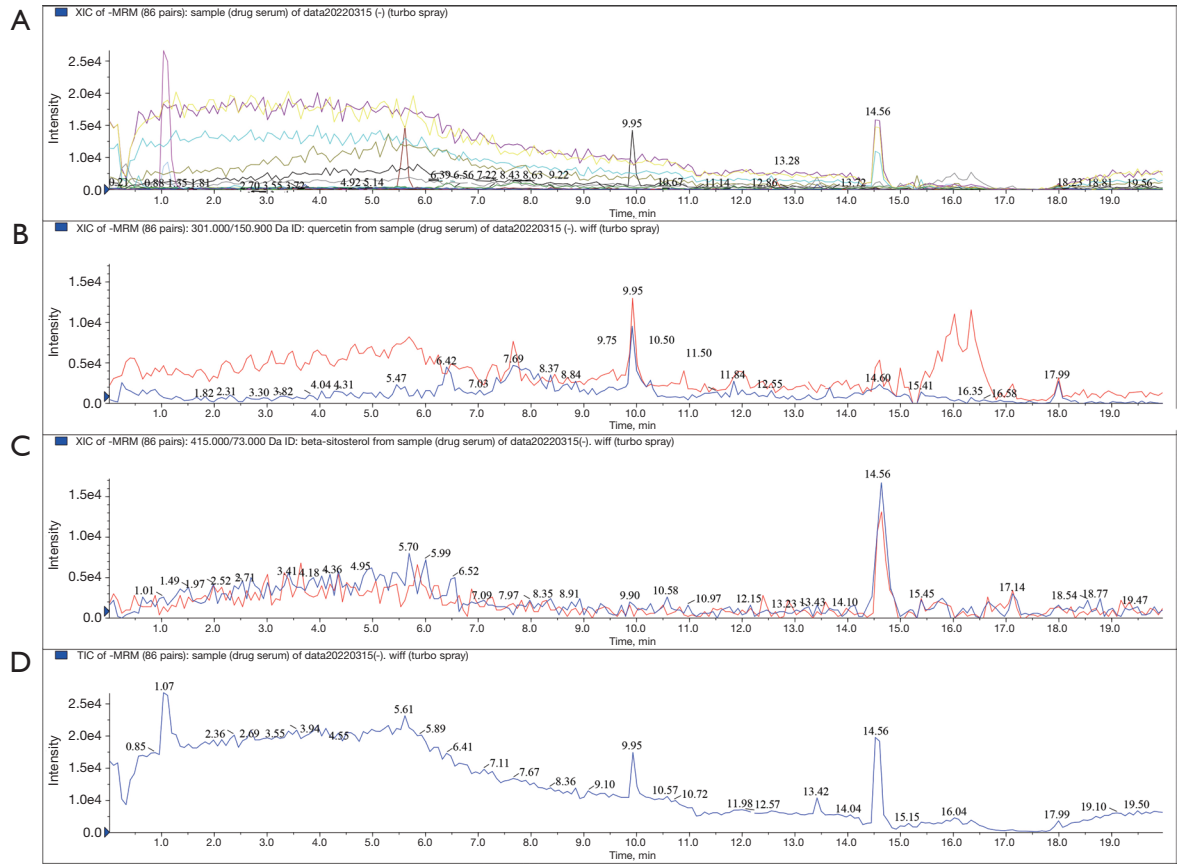

Figure 6 Ion chromatograms of drug serum by MRM in negative mode. (A) XIC of the drug serum; (B) XIC of quercetin; (C) XIC of beta-sitosterol; (D) TIC of drug serum. MRM, multiple reaction monitoring; XIC, extracted ion chromatogram; TIC, total ion chromatogram.

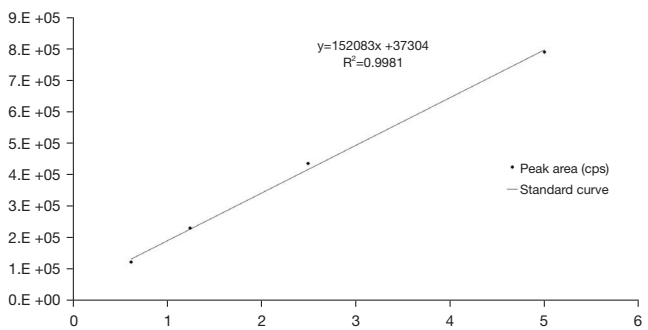

Figure 7 Standard curve of the ion pair from the quercetin standard in MRM−. The x-axis refers to the concentration of quercetin (μg/mL) and the y-axis refers to peak area (cps). MRM, multiple reaction monitoring.

reduced joint space was observed. Meanwhile, magnified scope (×200) showed alleviated lymphocyte infiltration in the synovium compared with the model group. In the Que-HD group (*Figure 10F*), regular scope (×40) showed that most of the articular cartilage was intact, with mild synovial hyperplasia. Compared with the model group, a clear joint space was observed. Meanwhile, magnified scope (×200) showed minor lymphocyte infiltration in the synovium compared with the model group.

Cytokine analysis

According to the results on day 28 (*Figure 11*), TNF-α, IL-1β, and IL-6 levels in the model group were obviously higher than those in the control group. After intervention

Table 4 Concentration and intra- and inter-day precision and accuracy of quercetin standards (0.625, 1.25, 2.5, and 5 μg/mL), the OD decoction, drug serum, and blank serum.

Validation sample (concentration, μg/g)	LLOQ	LQ	MQ	HQ	OD	Drug serum
Intra-day (mean ± SD)	0.62±0.04	1.28±0.08	2.54±0.09	4.74±0.4	3.15±0.08	0.95±0.05
Intra-day (%CV, n=5/day for 1 day)	0.06	0.06	0.03	0.08	0.02	0.05
Inter-day (mean ± SD)	0.64±0.05	1.34±0.08	2.54±0.08	4.85±0.12	3.13±0.08	0.98±0.03
Inter-day (%CV, n=1/day for 5 day)	0.07	0.06	0.03	0.02	0.03	0.03
Intra-day precision (%bias, n=5/day for 1 day)	5.64	6.8	3.38	5.14	NA	NA
Intra-day accuracy (%bias, n=5/day for 1 day)	5.78	6.21	3.05	6.72	1.96	7.2
Inter-day precision (%bias, n=1/day for 5 day)	6.55	8.91	2.78	3.15	NA	NA
Inter-day accuracy (%bias, n=1/day for 5 day)	5.86	4.83	2.79	2.27	2.15	2.9

OD, Oldenlandia diffusa; LLOQ, the lower limit of quantitation; LQ, low quantitation; MQ, middle quantitation; HQ, high quantitation; CV, coefficient of variation; SD, standard deviation.

Table 5 Record of stability and recovery of the OD decoction and drug serum.

RSD (%)	Stability in 4 ℃				Recovery		
Validation sample	0 h	6 h	12 h	24 h	80	100	120
OD	1.96	2.31	2.03	1.57	4.17	3.50	2.70
Drug serum	5.53	4.55	4.71	5.48	7.17	7.38	6.46

OD, Oldenlandia diffusa; RSD, relative standard deviation.

by OD, their expression was down-regulated, with IL-1β and IL-6 showing a significant difference compared with the model group ($P<0.05$). After intervention by Que-LD, cytokines were partially down-regulated, but showed no difference compared with the model group. After intervention by Que-MD or Que-HD, all cytokines were down-regulated, and showed significant differences compared with the model group ($P<0.05$). This effect was more significant in the Que-HD group compared with the OD group ($P<0.05$).

Evaluation of target proteins

According to the results of "Cytokine analysis", among the study of 3 different quantities of quercetin on CIA rats, we found that the high quantity exerted the most efficient effect on alleviating joint swelling, lymphocyte and pannus infiltration, synovial hyperplasia, articular cartilage damage, and inflammatory factors. Considering that quercetin might play its role by influencing MMP3 and CAV1 in the synovium, to verify this speculation, we chose Que-HD for subsequent interventions and conducted an analysis of the synovium by IHC (*Figure 12*) and ELISA (*Figure 13*), with intra-groups comparisons.

Immunohistochemical evaluation

As shown in *Figure 12A*,*12C*,*12E*,*12G*, MMP3 was hardly expressed in the control group (*Figure 12A*). In comparison, in the model group (*Figure 12C*), regular scope (×100) showed that MMP3 was highly expressed, and magnified scope (×400) showed that most of the expression was intercellular in the synovial matrix. In the OD group (*Figure 12E*) and Que-HD group (*Figure 12G*), regular scope (×100) showed that the expression of MMP3 was decreased compared with the model group, and magnified scope (×400) showed that this change was more significant in the Que-HD group. As shown in *Figure 12B*,*12D*,*12F*,*12H*), CAV1 was hardly expressed in the control group (*Figure 12B*). In comparison, in the model group (*Figure 12D*), regular scope (×100) showed that CAV1 was highly expressed, and magnified scope (×400) showed intracellular staining in the synovial cytoplasm. In the OD group (*Figure 12F*) and Que-HD group (*Figure 12H*), regular scope (×100) showed that the expression of MMP3 was decreased compared with the model group, and magnified scope (×400) showed that this change was more significant in the Que-HD group.

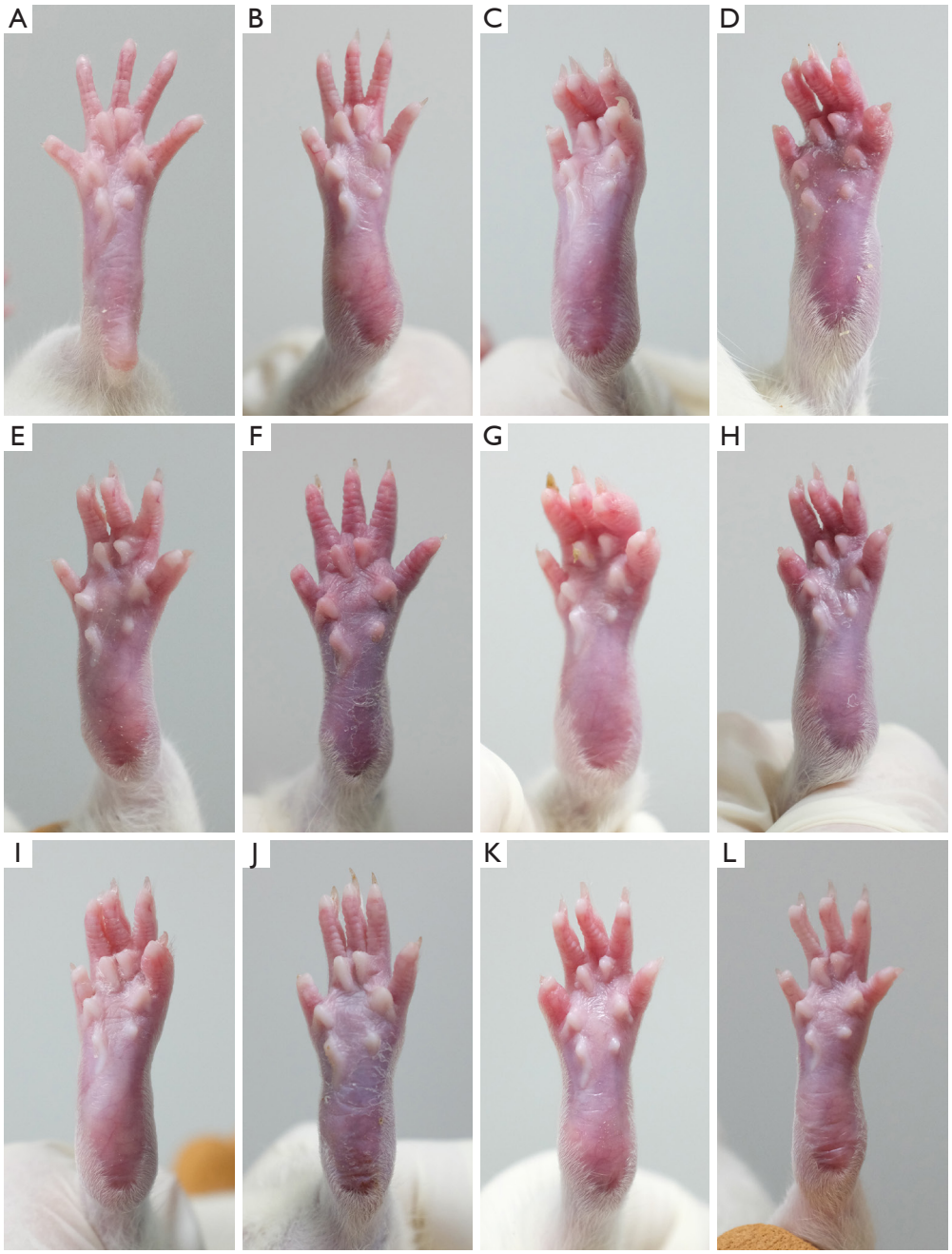

Figure 8 Morphological changes of the posterior limb in each group (A-L) from day 1 to 28. Control group (A). Model group on day 14 (B), 21 (C), and 28 (D). CIA rats treated with OD decoction (OD group) on day 21 (E) and 28 (F). CIA rats treated with Que-LD (Que-LD group) on day 21 (G) and 28 (H). CIA rats treated with Que-MD (Que-MD group) on day 21 (I) and 28 (J). CIA rats treated with Que-HD (Que-HD group) on day 21 on day 21 (K) and 28 (L). CIA, collagen induced arthritis; OD, Oldenlandia diffusa; Que-LD, quercetin in low dose; Que-MD, quercetin in medium dose; Que-HD, quercetin in high dose.

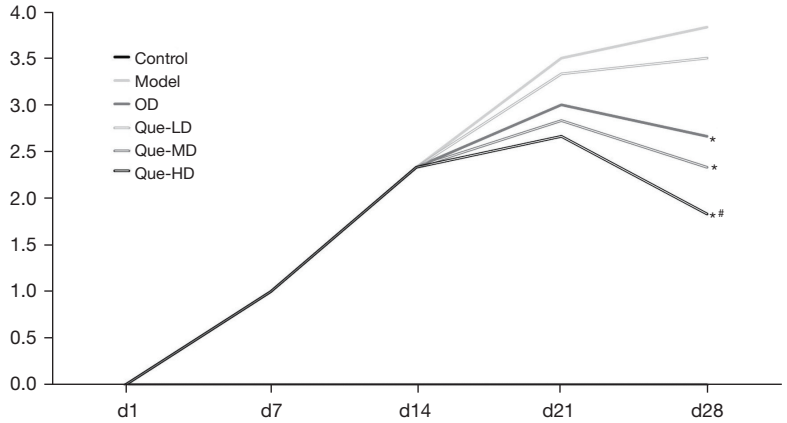

Figure 9 Means of arthritis index (AI) in each group, from day 1 to 28. In comparison with the model group (*, P<0.05); in comparison with the OD group (#, P<0.05). CIA rats treated with OD decoction (OD group). CIA rats treated with Que-LD (Que-LD group). CIA rats treated with Que-MD (Que-MD group). CIA rats treated with Que-HD (Que-HD group). CIA, collagen induced arthritis; OD, Oldenlandia diffusa; Que-LD, quercetin in low dose; Que-MD, quercetin in medium dose; Que-HD, quercetin in high dose.

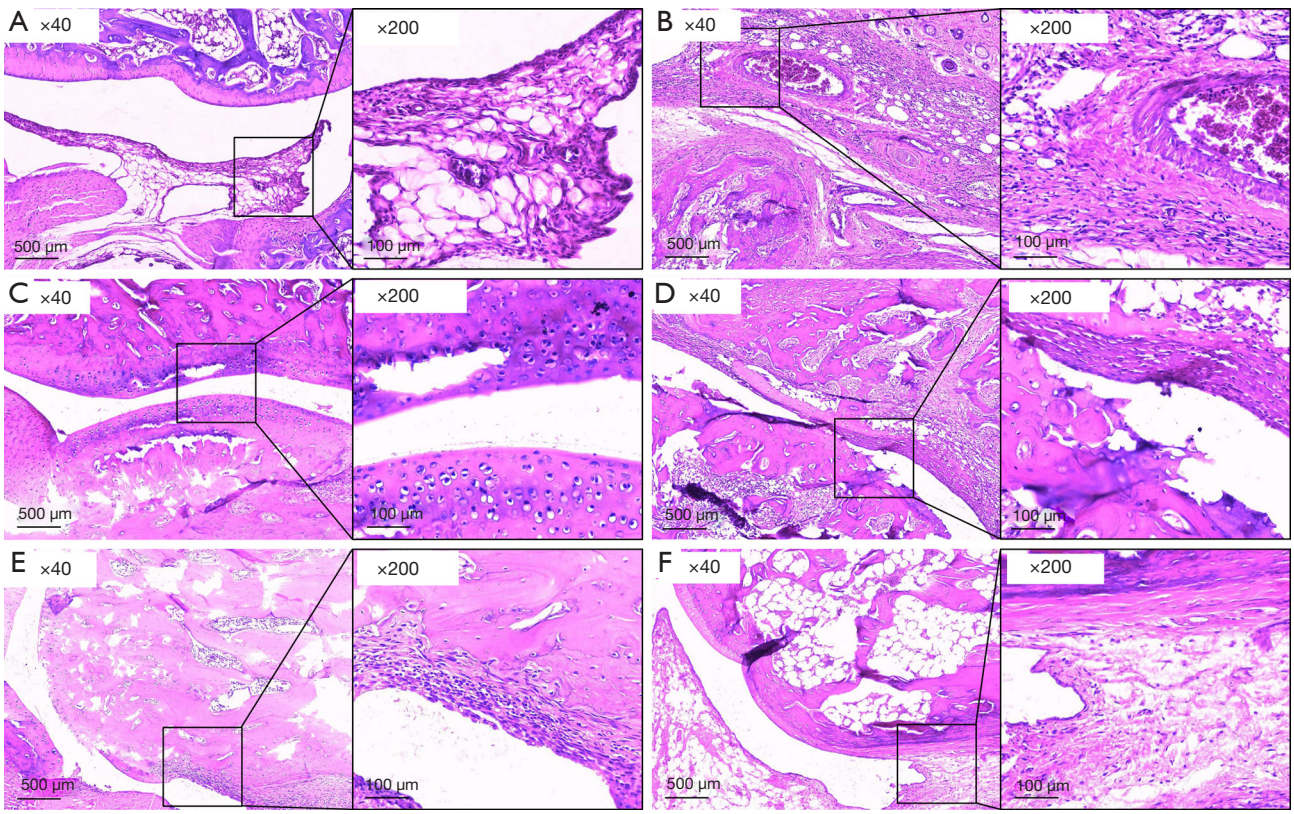

Figure 10 Histopathological changes (hematoxylin-eosin staining) of knee joint in each group (A-F) on day 28. In each image, left: regular scope (×40); right: magnified scope (×200). Control group (A). Model group (B). CIA rats treated with OD decoction (OD group) (C). CIA rats treated with Que-LD (Que-LD group) (D). CIA rats treated with Que-MD (Que-MD group) (E). CIA rats treated with Que-HD (Que-HD group) (F). CIA, collagen induced arthritis; OD, Oldenlandia diffusa; Que-LD, quercetin in low dose; Que-MD, quercetin in medium dose; Que-HD, quercetin in high dose.

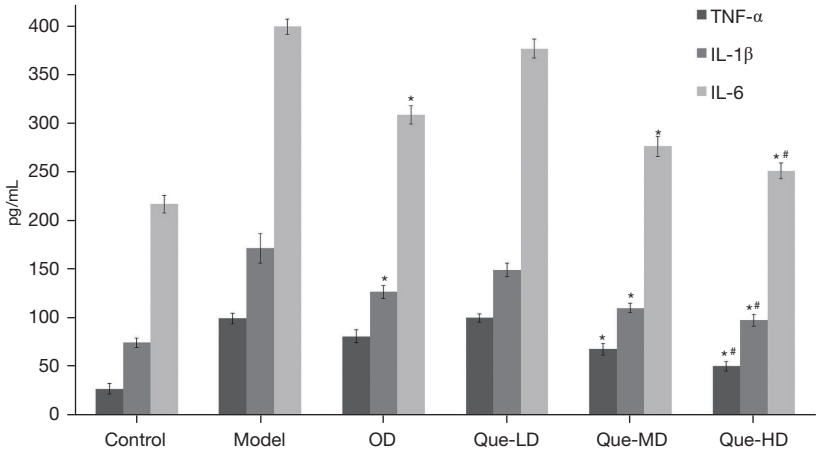

Figure 11 Serum cytokines (TNF-α, IL-1β, IL-6) in each group on day 28. In comparison with the model group (*, P<0.05); in comparison with the OD group (#, P<0.05). CIA rats treated with OD decoction (OD group). CIA rats treated with Que-LD (Que-LD group). CIA rats treated with Que-MD (Que-MD group). CIA rats treated with Que-HD (Que-HD group). CIA, collagen induced arthritis; OD, Oldenlandia diffusa; Que-LD, quercetin in low dose; Que-MD, quercetin in medium dose; Que-HD, quercetin in high dose.

ELISA evaluation

As shown in *Figure 13*, MMP3 (A) expression was significantly elevated in the model group compared to the control group (P<0.01), and after intervention with OD or Que-HD, the expression was significantly down-regulated compared with the model group (P<0.01). CAV1 (B) expression significantly increased in the model group compared to the control group (P<0.01), and after intervention by OD, the expression was slightly down-regulated and showed no difference compared with the model group. After intervention with Que-HD, CAV1 expression was down-regulated compared with the model group and OD group (P<0.05).

Discussion

Resent years, with the development of network technology, many scholars excavated the drug-target from database of pharmacology, and compared the results from database of disease, thus to find the potential drug-targets. The potential effective therapy could be achieved by synergistic multi-compound network pharmacology (20). Due to the characteristic of multi-compound of herbal medicine, this method is especially suitable for the study on TCM. Through network pharmacology analysis, Kai-Xin-San were found to participate in the treatment of Alzheimer's disease by regulating cholinergic cGMP/PKG pathway (21). Based on the clinical data of 125 patients infected with Covid-19, three effective TCM prescriptions were found through network pharmacology (22), and the relevant mechanism of action of EGCG as a potential therapeutic agent against COVID-19 were revealed. Among these studies, the underlying logic for this method is based on prediction, with uncertainties, and the results are in need of verification. In order to lay a solid result, in this study, we applied the quantitative proteomic analysis. Instead of searching through the database of RA, we directly emphasize the study point on synovial inflammation, which is synovium from different groups. To increase the accuracy of finding of targets, we applied iTRAQ. Compared with other proteomic analysis, iTRAQ is a technology which not only could filtrate DEPs by quantification and identification in accuracy, but also could analyze the relevant functions and pathways, with the advantages in high throughput, preferably connect to genomic or transcriptome data, and available for eight tags analysis (23). iTRAQ proteomic helped to reveal the variations in serum protein composition among seronegative RA, seropositive RA and healthy donor, and indicated new advanced diagnostic methods and precision treatment of RA (7). With the help of iTRAQ analysis, serotransferrin-related molecular mechanism was analyzed and might be a new direction to study RA (6). With these advantages, we intercepted the result of iTRAQ to disease database, forwardly increase the accuracy of proteomic result in this study.

In this study, with the help of iTRAQ based quantitative proteomics, we identified 67 DEPs from the synovium of

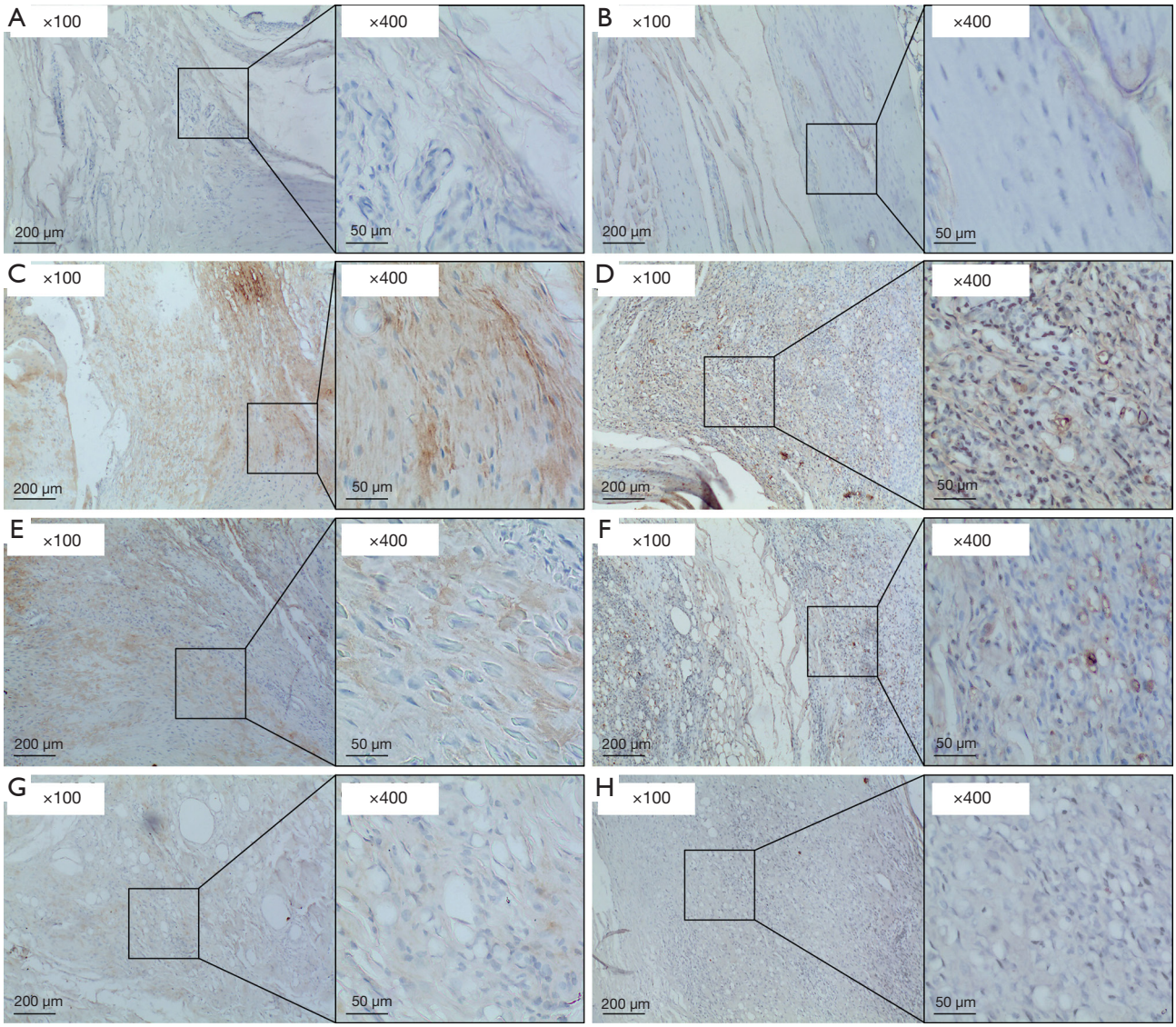

Figure 12 The expression of MMP3 (A,C,E,G) and CAV1 (B,D,F,H) in each group (immunohistochemistry staining) on day 28. In each image, left: regular scope (×100); right: magnified scope (×400). Control group (A,B). Model group (C,D). CIA rats treated with OD decoction (OD group) (E,F). CIA rats treated with Que-HD (Que-HD group) (G,H). CIA, collagen induced arthritis; OD, Oldenlandia diffusa; Que-HD, quercetin in high dose.

CIA rats with a fold change of 1.3 or –1.3, and these DEPs were associated with 34 significant canonical pathways. These DEPs and pathways were fundamental, and some of them might play key roles in the pathological processes of RA. With the help of network pharmacology, we filtrated the DEPs with several database in "synovitis, vasculitis", and found 2 DEPs, namely MMP3 and CAV1, which might be influenced by quercetin, one of the effective compounds of OD. Among all the pathways, 2 were relevant: MMP3 was involved in atherosclerosis signaling, while CAV1 was involved in caveolar-mediated endocytosis signaling.

MMP3 is a well-known proteinase generated and released by synovial fibroblasts in the joints (24). It has the ability of degrading multiple types of collagen, fibronectin, all actively involved in joint destruction in RA patients (25). MMP3 can also activate other MMPs such as MMP-1, MMP-7, and MMP-9 (26), indicating that MMP3 plays an important role in the inflammatory responses in RA. Among

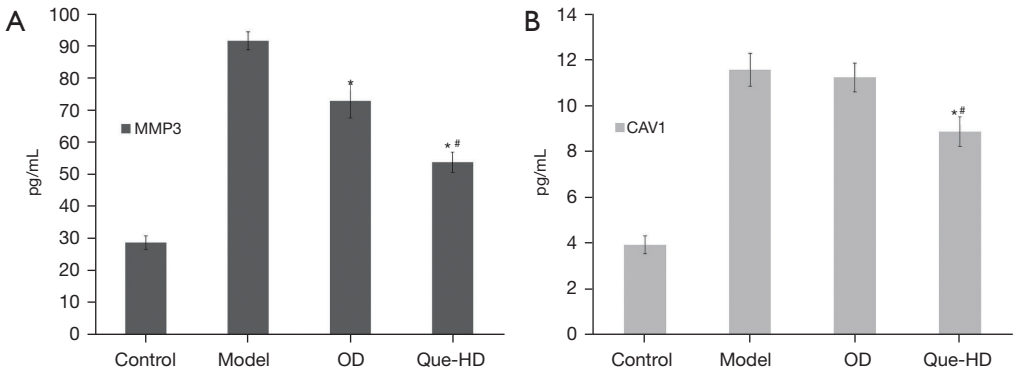

Figure 13 Synovial proteins MMP3 (A) and CAV1 (B) in each group on day 28. In comparison with the model group (*, P<0.05); in comparison with the OD group (#, P<0.05). CIA rats treated with OD decoction (OD group). CIA rats treated with Que-HD (Que-HD group). CIA, collagen induced arthritis; OD, Oldenlandia diffusa; Que-HD, quercetin in high dose.

these pathways, some are involved in atherosclerosis (27). For many years, atherosclerosis signaling was considered to have a close relationship with cardiovascular and cerebrovascular diseases. However, present studies indicate that atherosclerosis not only induces lipid metabolism dysfunction, but also inflammatory effects with involvement of the immune system. In the synovium of RA patients, as a typical pathological feature, synovial pannus always manifests in vascular proliferation and lymphocyte infiltration. A recent study indicated that inflammatory related atherosclerosis signaling played an important role in inflammatory vascular proliferation, with participation by MMP3. Thus far, mitogen-activated protein kinase (MAPK) signaling, toll-like receptor 4 (TLR4) signaling, and phosphatidylinositol 3-kinase and protein kinase B (PI3K/AKT) signaling has been reported. MAPK is expressed on the cell surface and can mediate the proliferation of vascular endothelial cells (28) and the expression of synovial inflammatory cytokines (29), which involves MMP3. TLR4 is an innate immune pattern recognition receptor, and studies showed that in atherosclerosis, TLR4 was involved in inflammatory responses through vascular pathological changes (30), and with the suppression of TLR4, the expression of MMP3 could be inhibited (31). The generation of pannus was accompanied by vascular smooth muscle cell proliferation, and the migration of vascular smooth muscle cells played an important role, as a study showed that the down-regulation of MMP3 could inhibit their migration (32).

CAV1 has been established as the principal structural protein of caveolae (33), one of the 3 members of the caveolin family (34). It is widely distributed in adipocytes, endothelial cells, and fibroblasts (35), and might play a role in the inflammatory response in RA (35). There have been rare direct reports of its inflammatory relevant effect in RA, but we found some indirect reports. A study showed that CAV1-knockout mice were characterized by a low-grade systemic pro-inflammatory status, with a moderate increase in IL-6, TNF-α, and IL-12 levels (36). CAV1 is also the costimulatory ligand for CD26, and ligation of CD26 by caveolin-1 could induce T-cell proliferation and NF-κB activation in a T-cell receptor CD3-dependent manner (37). The expression of CAV1 had a close relationship with cell proliferation and attenuated apoptosis in fibroblast-like synoviocytes (38). Caveolar not only played a role in the inflammatory response, but was also critical for caveolae-mediated endocytosis. A report showed that it is involved in cell signaling and endocytosis (39). Caveolar-mediated endocytosis between clathrin and G protein-coupled receptor kinase 2 (GRK2)/b-arrestin2 occurred in a GRK2-mediated receptor phosphorylation-dependent manner (40), while GRK2 is an important regulatory protein of the inflammatory immune response in RA. It was also found to be prominent in the activation of RAW 264.7 macrophages (41), which might induce inflammatory reactions, including RA (41).

According to network pharmacology analysis, we speculated that quercetin was OD's key compound, and it might play an anti-inflammatory role in synovitis by influencing MMP3 and CAV1 during the treatment of RA by OD. To verify this speculation, first, we quantified and qualified quercetin in OD and serum to prove it can be absorbed into blood after oral taken of the OD decoction, and found the concentration of quercetin in OD was 52.5 μg/g. Second, to choose the intervene dose of

quercetin, we calculated the regular dose of quercetin for rat was 0.28 mg/kg, based on it, we added the decuple and centuple doses of the regular one to intervene, and found Que-HD (28 mg/g) exerted the most significant effects on alleviating ankle swelling, skin redness, synovial hyperplasia, lymphocyte infiltration, articular cartilage damage, and serum cytokine factors. This result indicated that, in the treatment of RA by OD, quercetin may be its main effective compound and plays the most important role. quercetin is a flavonoid found in plants and has been verified to have anti-inflammatory effects (42). It could exert its effect by suppressing the clinical symptoms of arthritis by inhibiting the release of inflammatory cytokines (43) and NF-κB activity (44). It could also prevent the recruitment of macrophages (45) and neutrophils (46), as well as synoviocyte proliferation (47). Considering Que's anti-inflammatory characteristic, and the results from iTRAQ and network pharmacological analysis, we speculated quercetin, an active ingredient of OD, might exert the anti-inflammatory effect on RA by influencing MMP3 and CAV1. To verify the speculation, we further analyzed the impact of OD or quercetin on MMP3 and CAV1.

Presently, there are few reports of quercetin's effect on MMP3, and most of them are network pharmacology analyses (non-arthritis) and in need of verification. We found one experimental study which showed that quercetin could decrease the expression of MMP3 in serum (48), and could prevent joint inflammation (48) (mice immunized with type II collagen). A similar situation was found for CAV1, and recent studies showed that quercetin could suppress the expression of CAV1 in endothelial cells, thus alter the vascular permeability under oxidative stress (49), or exert an anti-atherosclerotic effect (50). None of them were related to the inflammatory response in arthritis. In this study, we intervened CIA model with OD or quercetin, and compared the expression of MMP3 and CAV1 in the knee joints of different groups. According to IHC, we found they were both up-regulated in the CIA model, which corresponded to the proteomics analysis results. Furthermore, MMP3 was mainly expressed in the synovial matrix, while CAV1 was expressed in the synovial cytoplasm. After intervention, both MMP3 and CAV1 were down-regulated by OD or Que. According to ELISA, we found that OD at the regular dose down-regulated the expression of MMP3 in the synovium of CIA rats, but had no significant effect on CAV1, while Que-HD had an effect on both. Additionally, we found that the centuple dose of quercetin exerted a better effect than OD at the regular dose. These findings indicated that OD has an anti-inflammatory effect on RA, and it might exert this effect by down-regulating MMP3 and CAV1 in the synovium through its main active compound Que. Herbal medicine has been applied in the treatment of RA for many years in China, a lot of experiment study of its effective compounds has been carried out, along with its mechanism. Total glucosides of paeony, the main active compound of Paeoniae Radix Alba are effective in the treatment of RA (51), can regulate intracellular pathways, such as the NF-κB, MAPK, and PI3K/Akt signal pathways (52). Tripterygium glycosides, the main active compound of Tripterygium has shown obvious anti-RA effects (53), and it can inhibit the PI3K/Akt/mTOR signaling pathway to alleviate inflammatory response (54). Both of them were currently and widely used in clinical treatment on RA.

After we completed this study, we reviewed the experiments and found that the main sample, synovium, was tiny in each rat. As we believed that CIA in rats could ideally match RA in humans, we are eager to induce CIA in other species, including human, *in vitro*. Nowadays, more and more scholars have performed experiments *in vitro*, such as fibroblast-like synoviocyte cultivation. We speculate that this method might be more direct, accurate, and efficient. Considering we did not verify our pathway results in this study, we are eager to conduct further experiments *in vitro* in the future.

Conclusions

In this study, we demonstrated that quercetin, a compound of OD, might have an anti-inflammatory effect on RA. OD could alleviate inflammatory responses in CIA rats and suppress the expression of MMP3 and CAV1 by its active compound quercetin, while MMP3 and CAV1 might play key roles in the inflammatory pathological processes in RA. Additionally, quercetin at a high dose showed significant effects. This information sheds light on the mechanism by which OD exerts its anti-inflammatory effect on RA.

Acknowledgments

Funding: This study was supported by the National Natural Science Foundation of China (No. 82004290).

Footnote

Reporting Checklist: The authors have completed the

ARRIVE reporting checklist. Available at https://atm.amegroups.com/article/view/10.21037/atm-22-3678/rc

Data Sharing Statement: Available at https://atm.amegroups.com/article/view/10.21037/atm-22-3678/dss

Conflicts of Interest: All authors have completed the ICMJE uniform disclosure form (available at https://atm.amegroups.com/article/view/10.21037/atm-22-3678/coif). The authors have no conflicts of interest to declare.

Ethical Statement: The authors are accountable for all aspects of the work in ensuring that questions related to the accuracy or integrity of any part of the work are appropriately investigated and resolved. Animal experiments were performed under a project license (No. SUDA20220613A01) granted by Ethics Committee of Soochow University, in compliance with the national guidelines for the care and use of animals.

References

1. Omidian S, Aghazadeh Z, Ahmadzadeh A, et al. Evaluating Mannuronic Acid Effect on Gene Expression Profile of Inflammatory Mediators in Rheumatoid Arthritis Patients. Iran J Allergy Asthma Immunol 2022;21:44-54.
2. Wang J, Yan S, Yang J, et al. Non-coding RNAs in Rheumatoid Arthritis: From Bench to Bedside. Front Immunol 2019;10:3129.
3. Krishna Priya EK, Srinivas L, Rajesh S, et al. Pro-inflammatory cytokine response pre-dominates immuno-genetic pathway in development of rheumatoid arthritis. Mol Biol Rep 2020;47:8669-77.
4. Luan J, Hu Z, Cheng J, et al. Applicability and implementation of the collagen-induced arthritis mouse model, including protocols (Review). Exp Ther Med 2021;22:939.
5. Chen J, Li J, Chen J, et al. Treatment of collagen-induced arthritis rat model by using Notch signalling inhibitor. J Orthop Translat 2021;28:100-7.
6. Chen J, Li S, Ge Y, et al. iTRAQ and PRM-Based Proteomic Analysis Provides New Insights into Mechanisms of Response to Triple Therapy in Patients with Rheumatoid Arthritis. J Inflamm Res 2021;14:6993-7006.
7. He Y, Lin J, Tang J, et al. iTRAQ-based proteomic analysis of differentially expressed proteins in sera of seronegative and seropositive rheumatoid arthritis patients. J Clin Lab Anal 2022;36:e24133.
8. He Z, Liu Z, Gong L. Biomarker identification and pathway analysis of rheumatoid arthritis based on metabolomics in combination with ingenuity pathway analysis. Proteomics 2021;21:e2100037.
9. Mashimo K, Ohno Y. Effect of Ethanol on Gene Expression in Beating Neonatal Rat Cardiomyocytes: Further Research with Ingenuity Pathway Analysis Software. J Nippon Med Sch 2021;88:209-19.
10. Yuan Y, Zhu C, Liu M, et al. Comparative proteome analysis of form-deprivation myopia in sclera with iTRAQ-based quantitative proteomics. Mol Vis 2021;27:494-505.
11. Xie FF, Wang HO, Cao QQ, et al. The effects of Oldenlandia diffusa water extract on glucose metabolism and inflammation level in rats with streptozotocin-induced gestational diabetes mellitus. Qual Assur Saf Crop 2022;14:24-30.
12. Zhu H, Liang QH, Xiong XG, et al. Anti-Inflammatory Effects of p-Coumaric Acid, a Natural Compound of Oldenlandia diffusa, on Arthritis Model Rats. Evid Based Complement Alternat Med 2018;2018:5198594.
13. Lv Y, Wang Y. Chemical constituents from Oldenlandia diffusa and their cytotoxic effects on human cancer cell lines. Nat Prod Res 2021. [Epub ahead of print]. doi: 10.1080/14786419.2021.1974434.
14. Zhou W, Lai X, Wang X, et al. Network pharmacology to explore the anti-inflammatory mechanism of Xuebijing in the treatment of sepsis. Phytomedicine 2021;85:153543.
15. Wang X, Wang ZY, Zheng JH, et al. TCM network pharmacology: A new trend towards combining computational, experimental and clinical approaches. Chin J Nat Med 2021;19:1-11.
16. Zhou Z, Chen B, Chen S, et al. Applications of Network Pharmacology in Traditional Chinese Medicine Research. Evid Based Complement Alternat Med 2020;2020:1646905.
17. Luo TT, Lu Y, Yan SK, et al. Network Pharmacology in Research of Chinese Medicine Formula: Methodology, Application and Prospective. Chin J Integr Med 2020;26:72-80.

18. Haleagrahara N, Miranda-Hernandez S, Alim MA, et al. Therapeutic effect of quercetin in collagen-induced arthritis. Biomed Pharmacother 2017;90:38-46.
19. Lim MA, Louie B, Ford D, et al. Development of the Digital Arthritis Index, a Novel Metric to Measure Disease Parameters in a Rat Model of Rheumatoid Arthritis. Front Pharmacol 2017;8:818.
20. Nogales C, Mamdouh ZM, List M, et al. Network pharmacology: curing causal mechanisms instead of treating symptoms. Trends Pharmacol Sci 2022;43:136-50.
21. Yi P, Zhang Z, Huang S, et al. Integrated meta-analysis, network pharmacology, and molecular docking to investigate the efficacy and potential pharmacological mechanism of Kai-Xin-San on Alzheimer's disease. Pharm Biol 2020;58:932-43.
22. Du A, Zheng R, Disoma C, et al. Epigallocatechin-3-gallate, an active ingredient of Traditional Chinese Medicines, inhibits the 3CLpro activity of SARS-CoV-2. Int J Biol Macromol 2021;176:1-12.
23. Vaudel M, Burkhart JM, Zahedi RP, et al. iTRAQ data interpretation. Methods Mol Biol 2012;893:501-9.
24. Guerrero S, Sánchez-Tirado E, Agüí L, et al. Simultaneous determination of CXCL7 chemokine and MMP3 metalloproteinase as biomarkers for rheumatoid arthritis. Talanta 2021;234:122705.
25. Lerner A, Neidhöfer S, Reuter S, et al. MMP3 is a reliable marker for disease activity, radiological monitoring, disease outcome predictability, and therapeutic response in rheumatoid arthritis. Best Pract Res Clin Rheumatol 2018;32:550-62.
26. Song HK, Noh EM, Kim JM, et al. Evodiae fructus Extract Inhibits Interleukin-1β-Induced MMP-1, MMP-3, and Inflammatory Cytokine Expression by Suppressing the Activation of MAPK and STAT-3 in Human Gingival Fibroblasts In Vitro. Evid Based Complement Alternat Med 2021;2021:5858393.
27. Ortiz G, Ledesma-Colunga MG, Wu Z, et al. Vasoinhibin is Generated and Promotes Inflammation in Mild Antigen-induced Arthritis. Endocrinology 2022;163:bqac036.
28. Wu HB, Wang ZW, Shi F, et al. Avβ3 Single-Stranded DNA Aptamer Attenuates Vascular Smooth Muscle Cell Proliferation and Migration via Ras-PI3K/MAPK Pathway. Cardiovasc Ther 2020;2020:6869856.
29. Behl T, Upadhyay T, Singh S, et al. Polyphenols Targeting MAPK Mediated Oxidative Stress and Inflammation in Rheumatoid Arthritis. Molecules 2021;26:6570.
30. Hovland A, Jonasson L, Garred P, et al. The complement system and toll-like receptors as integrated players in the pathophysiology of atherosclerosis. Atherosclerosis 2015;241:480-94.
31. Zhang M, Xue Y, Chen H, et al. Resveratrol Inhibits MMP3 and MMP9 Expression and Secretion by Suppressing TLR4/NF-κB/STAT3 Activation in Ox-LDL-Treated HUVECs. Oxid Med Cell Longev 2019;2019:9013169.
32. Ma L, Zhang L, Wang B, et al. Berberine inhibits Chlamydia pneumoniae infection-induced vascular smooth muscle cell migration through downregulating MMP3 and MMP9 via PI3K. Eur J Pharmacol 2015;755:102-9.
33. Robb R, Kuo JC, Liu Y, et al. A novel protein-drug conjugate, SSH20, demonstrates significant efficacy in caveolin-1-expressing tumors. Mol Ther Oncolytics 2021;22:555-64.
34. Hou K, Li S, Zhang M, et al. Caveolin-1 in autophagy: A potential therapeutic target in atherosclerosis. Clin Chim Acta 2021;513:25-33.
35. Trzybulska D, Olewicz-Gawlik A, Sikora J, et al. The effect of caveolin-1 knockdown on interleukin-1β-induced chemokine (C-C motif) ligand 2 expression in synovial fluid-derived fibroblast-like synoviocytes from patients with rheumatoid arthritis. Adv Clin Exp Med 2018;27:1491-7.
36. Codrici E, Albulescu L, Popescu ID, et al. Caveolin-1-Knockout Mouse as a Model of Inflammatory Diseases. J Immunol Res 2018;2018:2498576.
37. Ohnuma K, Uchiyama M, Yamochi T, et al. Caveolin-1 triggers T-cell activation via CD26 in association with CARMA1. J Biol Chem 2007;282:10117-31.
38. Li S, Jin Z, Lu X. MicroRNA-192 suppresses cell proliferation and induces apoptosis in human rheumatoid arthritis fibroblast-like synoviocytes by downregulating caveolin 1. Mol Cell Biochem 2017;432:123-30.
39. Tyrpak DR, Wang Y, Avila H, et al. Caveolin elastin-like polypeptide fusions mediate temperature-dependent assembly of caveolar microdomains. ACS Biomater Sci Eng 2020;6:198-204.
40. Zhang X, Zheng M, Kim KM. GRK2-mediated receptor phosphorylation and Mdm2-mediated β-arrestin2 ubiquitination drive clathrin-mediated endocytosis of G protein-coupled receptors. Biochem Biophys Res Commun 2020;533:383-90.
41. Phukan K, Devi R, Chowdhury D. Insights into Anti-Inflammatory Activity and Internalization Pathway of Onion Peel-Derived Gold Nano Bioconjugates in RAW 264.7 Macrophages. ACS Omega 2022;7:7606-15.
42. Costa ACF, de Sousa LM, Dos Santos Alves JM, et al. Anti-inflammatory and Hepatoprotective Effects of

Quercetin in an Experimental Model of Rheumatoid Arthritis. Inflammation 2021;44:2033-43.
43. Sun HT, Li JP, Qian WQ, et al. Quercetin suppresses inflammatory cytokine production in rheumatoid arthritis fibroblast-like synoviocytes. Exp Ther Med 2021;22:1260.
44. Ibrahim SSA, Kandil LS, Ragab GM, et al. Micro RNAs 26b, 20a inversely correlate with GSK-3 β/NF-κB/NLRP-3 pathway to highlight the additive promising effects of atorvastatin and quercetin in experimental induced arthritis. Int Immunopharmacol 2021;99:108042.
45. Luo M, Tian R, Yang Z, et al. Quercetin suppressed NADPH oxidase-derived oxidative stress via heme oxygenase-1 induction in macrophages. Arch Biochem Biophys 2019;671:69-76.
46. Yuan K, Zhu Q, Lu Q, et al. Quercetin alleviates rheumatoid arthritis by inhibiting neutrophil inflammatory activities. J Nutr Biochem 2020;84:108454.
47. Septembre-Malaterre A, Bedoui Y, Giry C, et al. Quercetin can reduce viral RNA level of O'nyong-nyong virus and resulting innate immune cytokine responses in cultured human synovial fibroblasts. Sci Rep 2021;11:6369.
48. Haleagrahara N, Hodgson K, Miranda-Hernandez S, et al. Flavonoid quercetin-methotrexate combination inhibits inflammatory mediators and matrix metalloproteinase expression, providing protection to joints in collagen-induced arthritis. Inflammopharmacology 2018;26:1219-32.
49. Kondo-Kawai A, Sakai T, Terao J, et al. Suppressive effects of quercetin on hydrogen peroxide-induced caveolin-1 phosphorylation in endothelial cells. J Clin Biochem Nutr 2021;69:28-36.
50. Kamada C, Mukai R, Kondo A, et al. Effect of quercetin and its metabolite on caveolin-1 expression induced by oxidized LDL and lysophosphatidylcholine in endothelial cells. J Clin Biochem Nutr 2016;58:193-201.
51. Jin T, Zhou Z, Zhou J, et al. The Potential Effects of Dielectric Barrier Discharge Plasma on the Extraction Efficiency of Bioactive Compounds in Radix Paeoniae Alba. Front Nutr 2021;8:735742.
52. Jiang H, Li J, Wang L, et al. Total glucosides of paeony: A review of its phytochemistry, role in autoimmune diseases, and mechanisms of action. J Ethnopharmacol 2020;258:112913.
53. Qian Q, Gao Y, Xun G, et al. Synchronous Investigation of the Mechanism and Substance Basis of Tripterygium Glycosides Tablets on Anti-rheumatoid Arthritis and Hepatotoxicity. Appl Biochem Biotechnol 2022;194:5333-52.
54. Hao F, Wang Q, Liu L, et al. Effect of moxibustion on autophagy and the inflammatory response of synovial cells in rheumatoid arthritis model rat. J Tradit Chin Med 2022;42:73-82.

(English Language Editor: C. Betlazar-Maseh)

Cite this article as: Zhu H, Xiong XG, Lu Y, Wu HC, Zhang ZH, Sun MJ. The mechanism of the anti-inflammatory effect of Oldenlandia diffusa on arthritis model rats: a quantitative proteomic and network pharmacologic study. Ann Transl Med 2022;10(20):1098. doi: 10.21037/atm-22-3678

